

# Lamina Cribrosa in Glaucoma: Diagnosis and Monitoring

Ricardo Y. Abe<sup>1,2</sup> · Carolina P. B. Gracitelli<sup>1,3</sup> · Alberto Diniz-Filho<sup>1,4</sup> · Andrew J. Tatham<sup>1,5</sup> · Felipe A. Medeiros<sup>1</sup>

Published online: 4 April 2015  
© Springer Science + Business Media New York 2015

**Abstract** The lamina cribrosa is the putative site of retinal ganglion cell axonal injury in glaucoma. Although histological studies have provided evidence of structural changes to the lamina cribrosa, even in early stages of glaucoma, until recently, the ability to evaluate the lamina cribrosa in vivo has been limited. Recent advances in optical coherence tomography, including enhanced depth and swept-source imaging, have changed this, providing a means to image the lamina cribrosa. Imaging has identified general and localized configurational changes in the lamina of glaucomatous eyes, including posterior laminar

displacement, altered laminar thickness, and focal laminar defects with spatial association with conventional structural and functional losses. In addition, although the temporal relationship between changes to the lamina cribrosa and glaucomatous retinal ganglion cell loss is yet to be elucidated, quantitative measurements of laminar microarchitecture have good reproducibility and offer the potential to serve as biomarkers for glaucoma diagnosis and progression.

**Keywords** Lamina cribrosa · Glaucoma · Diagnosis · Progression · Optical coherence tomography

This article is part of the Topical Collection on *Diagnosis and Monitoring of Glaucoma*.

✉ Felipe A. Medeiros  
fmedeiros@ucsd.edu

Ricardo Y. Abe  
ricardoabe85@yahoo.com.br

Carolina P. B. Gracitelli  
carolepm@gmail.com

Alberto Diniz-Filho  
adinizfilho@gmail.com

Andrew J. Tatham  
andrewjtatham@gmail.com

<sup>1</sup> Department of Ophthalmology, Hamilton Glaucoma Center, University of California, San Diego, San Diego, USA

<sup>2</sup> Department of Ophthalmology, University of Campinas, Campinas, Brazil

<sup>3</sup> Department of Ophthalmology, Federal University of São Paulo, São Paulo, Brazil

<sup>4</sup> Department of Ophthalmology and Otorhinolaryngology, Federal University of Minas Gerais, Belo Horizonte, Brazil

<sup>5</sup> Department of Ophthalmology, Princess Alexandra Eye Pavilion, University of Edinburgh, Edinburgh, Scotland

## Introduction

Glaucoma is a group of optic neuropathies characterized by progressive degeneration of retinal ganglion cells (RGCs), with resulting excavation of the optic nerve head (ONH), thinning of the retinal nerve fibre layer (RNFL), and loss of visual function [1]. Although the pathogenesis of glaucoma remains incompletely understood, the lamina cribrosa, a sieve like connective tissue structure through which RGC axons pass as they exit the eye, is thought to be the principal site of RGC vulnerability and the location of RGC axonal injury [2, 3]. Histological studies in human glaucomatous eyes have identified lamina cribrosa abnormalities; however, the temporal relationship between defects of the lamina cribrosa and glaucomatous neural damage is not well understood [4]. Recent study in non-human primates with experimental glaucoma have suggested that morphological changes to the lamina cribrosa might occur in the earlier stages of disease, implying that, identification of lamina cribrosa defects might be a useful diagnostic or prognostic marker [5]. Raised intraocular

pressure (IOP) is the major risk factor for glaucoma; however, many patients develop glaucoma with IOP within the normal range [6, 7]. It has been proposed that structural differences in the lamina cribrosa might be responsible for the differential effects of IOP within the tissues, contributing to individual susceptibility to IOP-mediated damage, and playing a significant role in the pathogenesis of visual damage in glaucoma [2, 8].

Located deep within the optic nerve head, until recently imaging *in vivo* of the lamina cribrosa has been limited. However, advances in optical coherence tomography (OCT) including enhanced depth imaging OCT (EDI-OCT) and swept-source OCT (SS-OCT) now provide a means for assessment of the lamina cribrosa. The purpose of this review is to appraise the recent literature regarding the potential role of lamina cribrosa imaging in the management of glaucoma.

### The Role of the Lamina Cribrosa in the Pathogenesis of Glaucoma

Approximately 1.2–1.5 million RGC axons converge at the ONH to exit the eye through the inner (i.e. Bruch's membrane opening) and outer (i.e. scleral) portions of the neural canal [9]. Within the scleral portion of the canal, the bundled axons pass through the lamina cribrosa, a meshwork of astrocyte-covered, capillary-containing connective tissue beams [10, 11]. Anatomically, the lamina cribrosa, which is located in the posterior sclera, helps to preserve a pressure gradient between the extraocular and intraocular spaces [12]. It is within the passage of the lamina cribrosa that RGC axons are thought to be most vulnerable to IOP-related stress and strain [13].

The ONH as a biomechanical structure is subject to acute and long-term changes to mechanical load including changes in morphology, microstructure, and material properties [14]. In glaucoma, these changes are thought to compromise RGC axon integrity as they pass through the lamina cribrosa, either directly due to axonal compression or indirectly as a consequence of impaired mechanical or nutritional support from glial cells and lamina cribrosa capillaries. In this biomechanical paradigm of glaucomatous optic neuropathy, the susceptibility of the ONH to IOP insult is a function of both the acute and long-term response of the constituent tissues to elevated IOP [15]. Eyes with a particular combination of connective tissue geometry, pliability, blood supply, and cellular reactivity may be more susceptible to damage at normal levels of IOP, whereas others may be less vulnerable to damage [15].

The lamina cribrosa has been shown to be subject to configurational changes in response to raised IOP. Previous study in non-human primates has shown that IOP-related damage to the load-bearing connective tissues of the ONH may occur

early in the course of experimental glaucoma [16]. Morphometric evaluation of the lamina cribrosa in human eyes has also shown that significant posterior displacement and bowing of the lamina can occur in response to IOP changes [17]. Another possible factor related to axonal damage in glaucoma is the trans-lamina pressure gradient (i.e. the difference between IOP and cerebrospinal fluid pressure).

The deformation and condensation of the lamina cribrosa has already been described by previous studies, indicating that the lamina cribrosa is thinner in glaucomatous than in control eyes [4, 18]. Therefore, the trans-lamina pressure difference occurs over a shorter distance, resulting in a steeper gradient. This gradient would be increased in eyes with thin laminae or in those in which the lamina becomes thin through the course of the disease, serving as a barrier to RGC axonal transport [19, 20]. Assuming that the steepness of this pressure gradient is of importance for the susceptibility of optic nerve fibres to glaucoma, the condensation of the lamina cribrosa in glaucomatous eyes may explain why eyes with advanced glaucoma have a higher risk for progression than eyes at a moderate stage of glaucoma [21]. Additionally, a study evaluating glaucoma patients and normal subjects who underwent cerebrospinal fluid pressure measurements from lumbar puncture showed that in glaucoma patients with normal IOP levels, the cerebrospinal fluid pressure is abnormally low, leading to an abnormally high trans-lamina cribrosa pressure difference [22].

A histological study evaluating glaucomatous eyes has suggested that regional difference in lamina cribrosa architecture might play an important role in determining the susceptibility to glaucomatous RGC axonal injury [4]. The study found the lamina cribrosa in glaucomatous eyes had larger pores in the superior and inferior poles with narrow connective tissue beams compared to the nasal and temporal regions of the lamina cribrosa. The low density of connective tissue support in these regions could lead to greater susceptibility for axonal damage and explain the clinical finding that glaucomatous eyes frequently show preferential loss of neural tissue in the superior and inferior portions of the ONH [3]. Although histological studies have provided evidence for the role of the lamina cribrosa in glaucoma pathogenesis, recent advances in imaging provide the opportunity to improve understanding through *in vivo* evaluation of the lamina cribrosa.

### In Vivo Evaluation of the Lamina Cribrosa

Since its introduction in 1991, OCT has rapidly evolved to become widely adopted for assessment of structural damage in glaucoma. [23]. Until a few years ago, clinically available OCT instruments used a technique referred to as time-domain OCT (TD-OCT) to obtain images of the

ocular fundus. Although RNFL thickness measurements obtained from TD-OCT have been shown to discriminate normal eyes from those with glaucoma, this technology was limited by a suboptimal resolution and slow scans acquisition times [24, 25]. The introduction of spectral domain (SD-OCT) improved resolution and scan acquisition time compared to TD-OCT, leading to better reproducibility and accuracy in quantifying structural damage in glaucoma [26]. However, ability to visualize structures such as the choroid and lamina cribrosa remained limited due to poor signal penetration through the retinal pigment epithelium and choroid, light beam defocus at the level of the choroid relative to the retina, inadequate contrast between structures of critical interest, and limited lateral resolution of the scan [27–29].

SD-OCT does not adequately resolve deep anatomical structures as it measures depth information using a frequency pattern. When the eye is illuminated and backscattered light is captured by the interferometer, the deeper a structure, the higher its delay [30]. The “zero-delay” line is a reference point set by the software where the image capture is optimal, typically the vitreous and retina junction. In order to overcome this issue, enhanced depth imaging (EDI) was developed by Spaide et al. [31]. Using a commercially available SD-OCT device (Spectralis, Heidelberg Engineering, Heidelberg, Germany), Spaide et al. placed the OCT closer to the eye than in normal practice, thereby obtaining an inverted image with the most tightly focused illumination more posteriorly located at the level of the choroid and inner sclera. This technology has been recently used to evaluate not only choroid but also the lamina cribrosa [32, 33]. Figure 1 shows EDI-OCT of the ONH images of the right eye from a glaucoma patient.

The wavelength of light used in an OCT system affects image resolution, and when penetration depth increases, the image resolution and signal strength decrease. Commonly used SD-OCT devices utilize wavelengths in the range of 840–880 nm [34]. A recently developed OCT technology, swept-source OCT (SS-OCT), uses 1- $\mu\text{m}$  wavelength, which allows higher penetration with minimum light absorption and dispersion by the vitreous, providing improved imaging of deeper ONH structures [35, 36]. Figure 2 compares imaging with EDI-OCT and SS-OCT in the right eye of a glaucoma patient.

Recently, another technology used to evaluate the lamina cribrosa is adaptive optics. This system uses a wavefront sensor to measure ocular aberrations, for example, those induced by the lens and cornea. A deformable mirror or a spatial light modulator is then used to compensate for measured aberrations and improve image quality [37, 38]. Adaptive optics can correct ocular aberrations in real time and be combined with OCT or scanning laser ophthalmoscopy (SLO) [39–41].

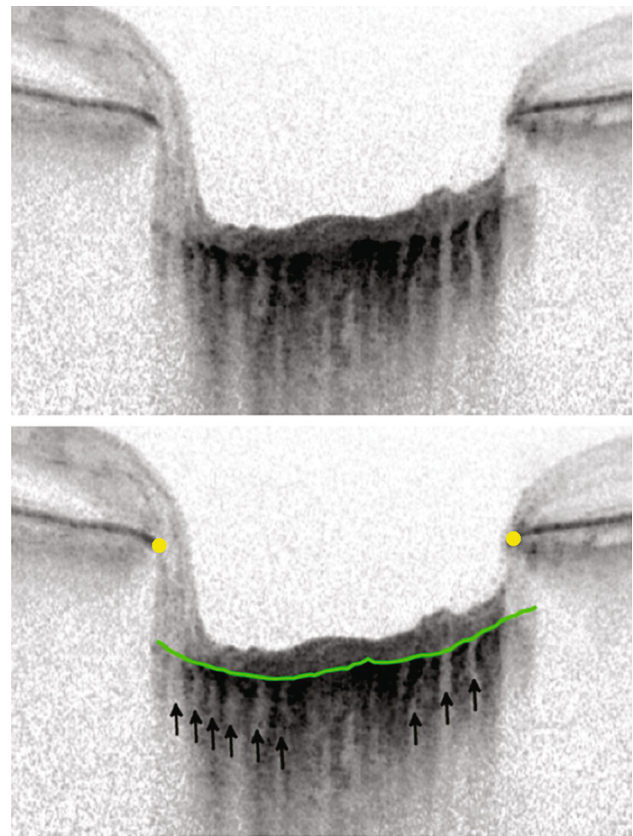


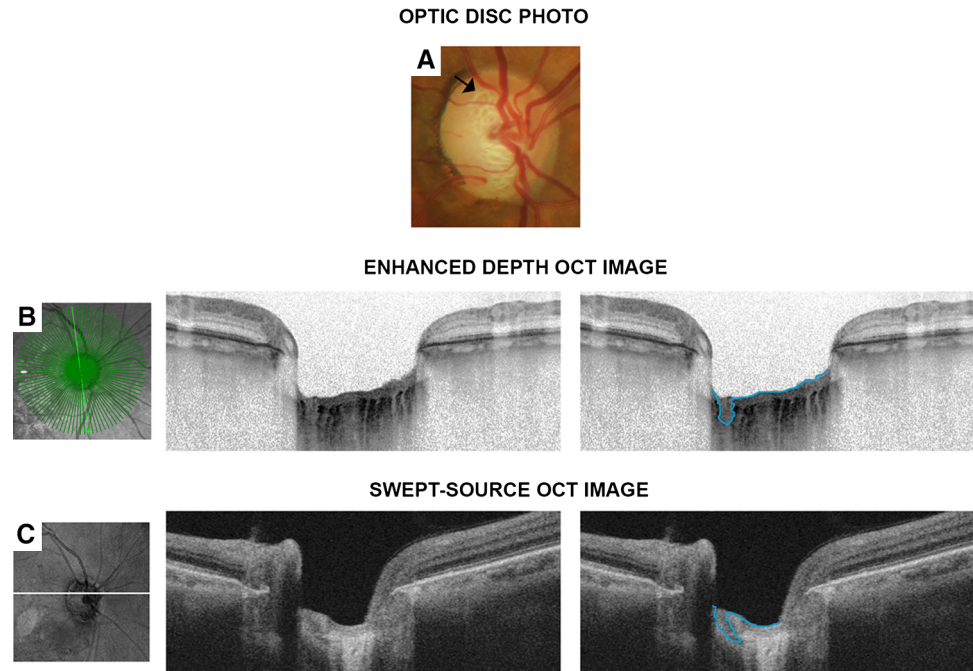
**Fig. 1** Enhanced depth imaging with spectral-domain optical coherence tomography (Spectralis, Heidelberg Engineering, Heidelberg, Germany) images of the optic nerve head of the right eye of a patient with glaucoma (the *green line* delineates the anterior lamina cribrosa, the two *yellow circles* show the Bruch's membrane opening, and the *arrows* indicate the lamina pores) (Color figure online)

The use of EDI-OCT, SS-OCT, and adaptive optics-OCT or -SLO has allowed improved in vivo evaluation of the lamina cribrosa, including examination of lamina posterior displacement, lamina cribrosa thickness, focal defects, and three-dimensional (3D) microstructure (Table 1). The relationship between these parameters and ageing, severity of glaucoma and their response to different IOP levels are crucial to determine whether the lamina cribrosa can truly provide useful information for glaucoma diagnosis and monitoring or if it is able to predict glaucomatous damage better than current imaging and visual functional devices.

### Posterior Displacement and Thickness of Lamina Cribrosa

A common feature observed in glaucomatous eyes and those with raised IOP has been posterior displacement of the lamina cribrosa. Yan et al. described posterior lamina cribrosa displacement following acute IOP elevation in human cadaver eyes [17], and recent studies have observed

**Fig. 2** Optic disc photograph from the right eye of a glaucoma patient with the arrow showing a clinically visible lamina cribrosa defect (a). Radial scans from the enhanced depth imaging with spectral-domain optical coherence tomography (EDI-OCT) device (Spectralis, Heidelberg Engineering, Heidelberg, Germany) showing unmarked image and manually marked focal defect on the superior region of the optic disc (b). The axial scans show the same defect on the superior region of the optic nerve using the swept-source optical coherence tomography (SS-OCT) device (Deep Range Imaging; Topcon, Japan) (c)



similar findings *in vivo*. Park et al. compared the morphology and position of lamina cribrosa between glaucomatous and normal eyes using EDI-OCT [42]. They found posterior bowing and sliding of the laminar insertion, with localized deformation of the lamina cribrosa in those with glaucoma. The regions of laminar deformation showed good spatial correlation to regions of RNFL and visual field defects. Another study demonstrated that the central and mid-peripheral portions of the lamina cribrosa were located more posteriorly in glaucomatous compared to normal eyes, as well as in eyes with visual field defects compared to fellow eyes with no visual field defects [43]. These results support the concept of the posterior lamina cribrosa displacement in glaucoma patients.

Previous studies have suggested that elevated IOP could disrupt the structural organization of the lamina cribrosa, interrupting the axoplasmic flow; however, age might affect structural stiffness or compliance of the ONH and peripapillary sclera and therefore contribute to individual responses to a given level of IOP exposure [4, 18, 44]. In fact, Ren et al. investigated if the lamina would be less posteriorly deformed in older eyes than in younger eyes under a similar level of IOP exposure. Their findings suggested that the lamina cribrosa might be shallower in older patients, and this age-related difference increases with disease severity [44].

Seo et al. investigated lamina cribrosa depth in 300 normal eyes using EDI-OCT. Lamina cribrosa depth was measured using the Bruch's membrane opening level as the reference. The results showed a wide variation in normal lamina cribrosa depth, with a mean of  $402 \pm 101.46 \mu\text{m}$

(range 193.08–826.81  $\mu\text{m}$ ) [45]. Males had significantly deeper-located lamina cribrosa than females, in agreement with a previous observation that males tend to have a larger mean cup depth than females [46]. Axial length was also found to have a negative correlation with lamina cribrosa depth. In myopic eyes, increasing axial during childhood can result in posterior migration of the temporal sclera and flattening. Consequently, the optic nerve is pulled temporally, and the connection between the temporal disc and the sclera also becomes flattened, leading to an oblique (or tilted) appearance of the optic disc [47]. It is likely that these changes are associated with shallowing of lamina cribrosa depth. Although the position of the lamina cribrosa may change during the glaucomatous process, the wide variation in lamina cribrosa depth in normal patients may limit the ability of lamina cribrosa measurements for diagnostic purposes, especially if factors such as axial length are not also taken into account. For this reason, future studies with longitudinal measurements over time may provide a more useful index for glaucoma management.

The thickness of the lamina cribrosa may also have a significant impact on the biomechanics of the ONH, playing an important role in the pathogenesis of glaucomatous optic nerve damage [48, 49]. Previous reports have suggested that the lamina cribrosa is thinner in glaucomatous eyes, and thinning becomes more pronounced as the disease progresses. [50]. Park et al. investigated the ability of laminar thickness versus RNFL measurements in diagnosing glaucoma with EDI-OCT in a cross-sectional study [33]. The mean laminar thickness differed significantly

**Table 1** Summary of studies about the relationship between the lamina cribrosa parameters and glaucoma

Study	Parameter	Subjects	Eyes	Device	Segmentation	Summary
Furlanetto et al. [43•]	Posterior displacement	Glaucoma Normal	47 57	EDI-OCT	Manual	The central and mid-peripheral lamina cribrosa is located more posteriorly in glaucomatous than in normal eyes
Ren et al. [44]	Posterior displacement	Suspect Glaucoma	221	SD-OCT	Manual	Older eyes have shallower lamina cribrosa comparing to younger eyes at a given level of visual field loss
Seo et al. [45•]	Posterior displacement	Normal	300	EDI-OCT	Manual	Lamina cribrosa depth is associated with sex and axial length. No differences were found between right and left eyes within same subject
Park et al. [33]	Thickness	Glaucoma Normal	144 65	EDI-OCT	Manual	Diagnostic capability of lamina cribrosa thickness is similar to RNFL thickness in glaucoma patients
Park et al. [51]	Thickness	Glaucoma	32	EDI-OCT SS-OCT	Manual	Detection of the posterior border of the lamina cribrosa was similar for the EDI and SS-OCT
You et al. [53]	Focal defects	Glaucoma	185	EDI-OCT	Manual	Lamina cribrosa defects were associated with neuroretinal rim loss and acquired pit of the ONH
Park et al. [55]	Focal defects	Glaucoma	148	EDI-OCT	Manual	Significant association between disc haemorrhage, NTG diagnosis, and advanced glaucoma with focal lamina cribrosa defects.
Tatham et al. [54]	Focal defects	Glaucoma Normal	20 40	EDI-OCT	Manual	Focal lamina cribrosa defects can be detected with EDI-OCT in glaucomatous eyes with localized RNFL defects
Lee et al. [56]	Focal defects	Glaucoma	81	EDI-OCT	Manual	The focal lamina cribrosa defect was spatially correlated with the location of disc haemorrhage
Nadler et al. [65••]	3D microarchitecture	Glaucoma Normal	16 14	SS-OCT Adaptive-OCT	Automated	Automated segmentation performed comparably to manual segmentation with the advantage of faster image evaluation
Wang et al. [67]	3D microarchitecture	Glaucoma Normal	49 19	SS-OCT	Automated	Larger beam thickness to pore diameter ratios and higher pore diameter standard deviations were found in glaucoma patients
Wang et al. [68]	3D microarchitecture	Glaucoma Suspect Normal	19 12 8	SS-OCT	Automated	Automated segmentation of the lamina cribrosa demonstrated high reproducibility for lamina cribrosa parameters using SS-OCT
Nadler et al. [66]	3D microarchitecture	Glaucoma Suspect Normal	12 5 9	Adaptive-OCT	Automated	3D lamina cribrosa microarchitecture parameters obtained by Adaptive-OCT have good repeatability

OCT optical coherence tomography, EDI enhanced depth imaging, SS swept source, RNFL retinal nerve fibre layer, NTG normal tension glaucoma, 3D three dimensional, ONH optic nerve head

( $P < 0.001$ ) between the glaucoma ( $215.41 \pm 38.96 \mu\text{m}$ ) and control ( $349.08 \pm 23.34 \mu\text{m}$ ) groups, and the mean laminar thickness was significantly greater ( $P < 0.001$ ) in the primary open angle glaucoma (POAG) group compared with the normal tension glaucoma (NTG) group ( $174.36 \pm 24.41 \mu\text{m}$ ). Laminar thickness had good diagnostic accuracy to discriminate eyes with POAG from controls with an area under the receiver operating characteristic (ROC) curve of 0.941 (0.931–0.952) for early POAG. For diagnosing early NTG, the ROC curve area was 0.981 (0.968–0.992). These numbers compared favourably to the performance of RNFL thickness. In fact, average RNFL thickness had an ROC curve areas of 0.928 (0.910–0.944) and 0.941 (0.925–0.957) for detecting early POAG and NTG, respectively. Figure 3 illustrates the comparison between the right eye of glaucoma patient (with localized RNFL defect, thinning of the lamina and also, a focal defect in the lamina cribrosa) and a healthy subject.

Inter-observer reproducibility of laminar thickness measurements has also been investigated, with reported inter-observer intraclass correlation coefficients of 0.906 and 0.907 when measured by EDI-OCT and SS-OCT,

respectively. These results suggest that the detection rate of the posterior border of the lamina cribrosa was similar for the two devices, with good reproducibility [51].

### Focal Defects of the Lamina Cribrosa

In addition to changes in lamina cribrosa depth and thickness, previous studies have suggested that focal lamina cribrosa defects may be important structural features in glaucoma and could potentially serve as biomarkers for glaucomatous visual field loss [3, 52]. Figure 4 illustrates the right eye of a glaucoma patient with localized RNFL defect and a focal defect in the lamina cribrosa. A cross-sectional study investigated the association between focal lamina cribrosa defects and neuroretinal rim thinning/notching and acquired pits of the optic nerve [53]. A laminar hole was defined as a localized discontinuity of lamina cribrosa tissue, whereas laminar disinsertion was defined as a posteriorly displaced laminar insertion. Both types of lamina cribrosa defects were required to be at least 100  $\mu\text{m}$  in diameter. By superimposing the images of the 3-dimensionally reconstructed focal

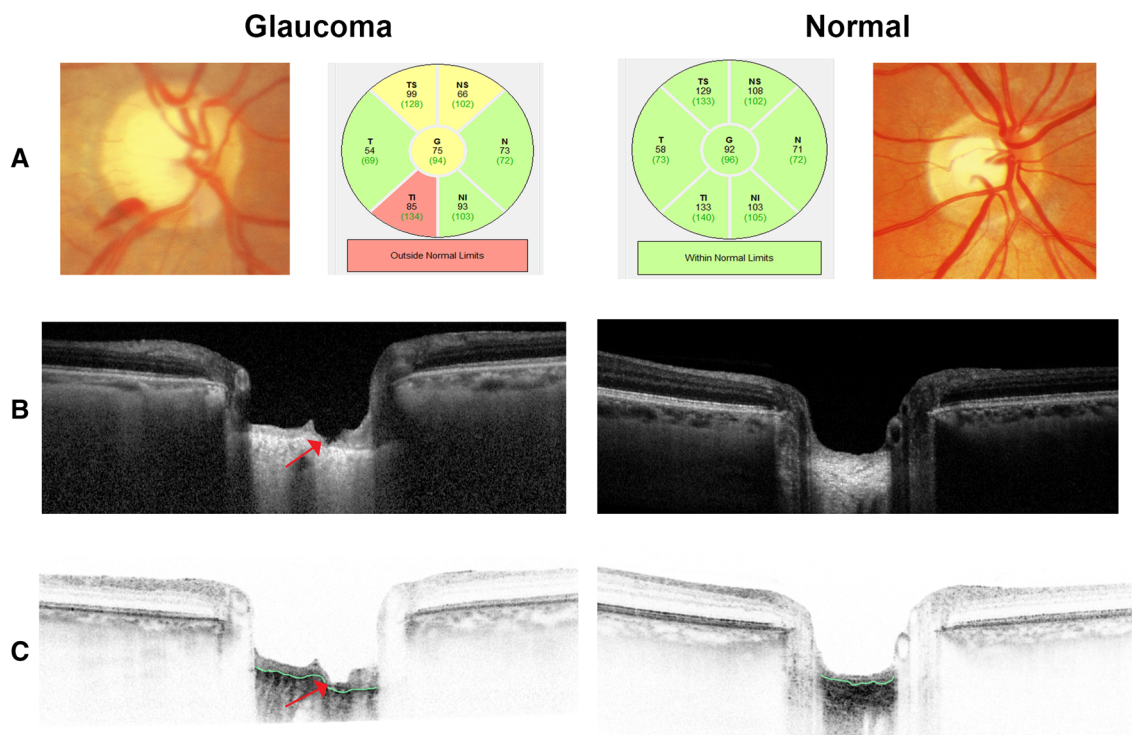
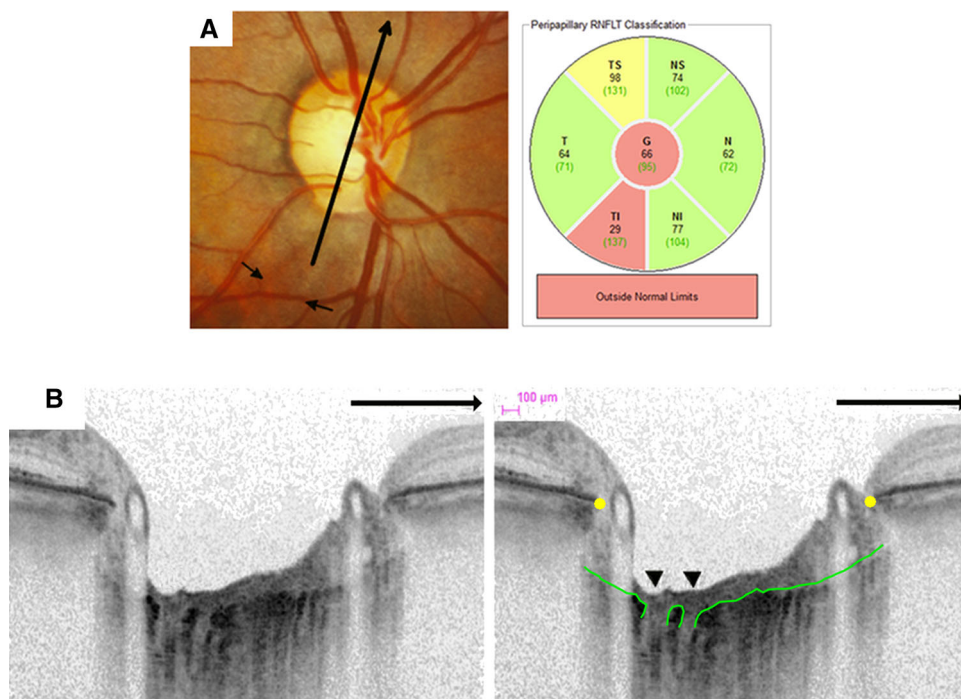


**Fig. 3** Series of optic disc photographs, optical coherence tomography (OCT) measurement of circumpapillary retinal nerve fibre layer (RNFL) thickness (a) and enhanced depth imaging OCT (Spectralis, Heidelberg Engineering, Heidelberg, Germany) images of the right eye of a glaucoma patient and a healthy subject (b, c). A disc

haemorrhage on optic disc photography and a localized RNFL defect on OCT are visible. Radial line EDI-OCT images shows that the lamina thickness is thinner (the green line delineating the anterior lamina cribrosa) in the glaucoma patient and highlight a focal defect in the lamina cribrosa (red arrow head) (Color figure online)

**Fig. 4** Optic disc photographs, optical coherence tomography (OCT) measurement of circumpapillary retinal nerve fibre layer (RNFL) thickness (a) and enhanced depth imaging OCT images (Spectralis, Heidelberg Engineering, Heidelberg, Germany) of the right eye of a patient with glaucoma (b). A localized RNFL defect is visible on optic disc photography (small arrows) with corresponding inferotemporal RNFL thinning on OCT. Radial line EDI-OCT images were taken through the optic nerve head with the direction of the scans shown on the optic disc photographs (large arrows). EDI-OCT shows two focal defects in the lamina cribrosa (arrow heads) in the region of the visible RNFL defect



lamina cribrosa defects (i.e. laminar holes or disinsertions) and optic disc photographs, they found that 33 % of the focal lamina defects identified on EDI-OCT imaging were clinically visible through the photographs, and also, the focal lamina defect corresponded to acquired pits of the optic nerve. The remaining lamina defects corresponded to neuroretinal rim thinning/notching, but these lamina defects were not visible in the photographs. These results suggest focal lamina cribrosa defects may be associated with neuroretinal rim loss and acquired pits of the optic nerve and these defects can be visualized more effectively using EDI-OCT than optic disc photographs. One limitation of this study was the exclusion of 54 from 239 eyes initially included because of incomplete horizontal or vertical EDI-OCT images or due to poor-quality EDI-OCT images secondary to media opacity, irregular tear film or poor patient cooperation. Moreover, defining the cutoff for lamina cribrosa defect in 100  $\mu$ m may have underdiagnosed some patients with smaller laminar defects.

Tatham et al. investigated the frequency and location of lamina defects and their relationship with RNFL defects using EDI-OCT [54]. Their study demonstrated that focal lamina cribrosa defects might be detected in vivo using EDI-OCT in glaucomatous eyes with localized RNFL defects, with good inter-observer agreement [54]. At least one focal lamina cribrosa defect was detected in 75 % of the eyes with a localized RNFL defect, suggesting that focal lamina cribrosa defects might predispose to localized loss of RGC axons passing through the damaged sector. In another investigation, eyes with focal laminar defects were

found to have significantly higher prevalence of disc haemorrhages (25 vs. 6 %), normal tension glaucoma (33 vs. 9 %), and worse visual field mean deviation ( $-14.12$  vs.  $-9.58$  dB) compared to eyes without focal defects [55]. Lee et al. also investigated whether disc haemorrhages were associated with structural alteration of the peripheral lamina cribrosa assessed by EDI-OCT [56]. Lamina alterations were found in 88.9 % of eyes with disc haemorrhage versus 11.1 % of eyes without haemorrhage, suggesting that structural changes in the lamina may be spatially associated with disc haemorrhage [56]. However, it is important to note that in the study only the temporal lamina was evaluated, since visualization of the other regions was obscured by thick neuroretinal rim or by central retinal vessels. In addition, approximately 25 % of the initial sample was excluded due to poor visualization of lamina structures.

A retrospective observational study evaluated the association between lamina cribrosa defects and glaucomatous visual field progression [57]. The study enrolled patients with at least 5 visual field tests using standard automated perimetry and pointwise linear regression analysis was used to define progression [58]. The EDI-OCT images were reviewed for the presence of laminar holes and laminar disinsertions. Visual field progression occurred in 47 % of eyes with focal lamina cribrosa defects versus only 25 % of eyes without lamina cribrosa defects ( $P = 0.003$ ). Although these findings suggest that laminar defects may be associated with risk of progression, it is important to emphasize that the retrospective design of the study does

not allow establishing a causal relationship. It is possible that the lamina defect could be just an epiphenomenon related to glaucoma progression. These studies, however, open exciting venues for the evaluation of the role of the lamina cribrosa as a potential site for assessment of risk of development and progression in glaucoma.

### Microarchitecture of the Lamina Cribrosa

Different studies have also attempted to evaluate the microarchitecture of the lamina cribrosa in glaucoma [59–62]. Initial studies were performed using colour disc photography or SLO [59–62], however, the low resolution and poor visualization of the lamina pores limited proper evaluation of microarchitecture with these techniques. Improvement in visualization of lamina cribrosa microarchitecture has been achieved with SS-OCT and adaptive optics technology. For example, Akagi et al. evaluated lamina cribrosa pores using adaptive optics-SLO from 40 eyes (20 normal and 20 glaucomatous), concluding that pore area was significantly larger in glaucomatous subjects than in normal subjects and was significantly associated with cup/disc ratio [38]. Changes in the lamina pore dimensions may be attributable to various factors such as tissue remodelling and mechanical deformation of the lamina cribrosa. Also, this study was the first to report that lamina cribrosa pore area was also associated with axial length ( $P < 0.001$ ). However, the reason for this association is currently uncertain, although the elongation of the axial length may lead to a lateral extension of the lamina [3].

Recently, a combination of adaptive optics with SD-OCT has also allowed 3D in vivo imaging of the lamina cribrosa [63, 64]. Using this technique, an automated segmentation method for lamina cribrosa microstructure evaluation was developed [65••]. The automated segmentation scans of the lamina cribrosa were compared against manual segmentations of coronal slices of the lamina cribrosa, using two different OCT technologies (Prototypes of SS-OCT and a adaptive optics-OCT) [65••]. The study evaluated 16 glaucoma patients and 14 normal subjects and adopted a manual segmentation of the lamina cribrosa as the gold-standard reference. Average sensitivity and specificity of the automated segmentation for glaucoma detection was 82.3 and 91.0 for SS-OCT and 80.1 and 88.0 % for adaptive optics-OCT, respectively. These results show that an automated method for 3D lamina cribrosa structure segmentation can perform similarly to manual segmentation with the advantage of being 100 times faster. Therefore, the automated algorithm permits rapid 3D segmentation for use in broader population studies of lamina cribrosa microarchitecture [65••].

The same group has investigated repeatability of 3D lamina cribrosa microarchitecture scans using the automated segmentation in a prototype adaptive optics-OCT [66]. Lamina cribrosa segmentations were used to quantify pore and beam structure through several global microarchitecture parameters. Similar measurements from pore and beam structure were observed on repeated scans, demonstrating high repeatability with imprecisions of less than 4.7 %, suggesting that quantitative measurements of lamina cribrosa microarchitecture obtained from adaptive optics-OCT automated segmentation might be used for assessing longitudinal changes in the lamina cribrosa over time. However, this study also showed measurement of the whole lamina cribrosa was often not possible, due to difficulty of visualization of the peripheral lamina cribrosa, which was obstructed by neural tissue, vasculature, and peripapillary sclera.

Automated segmentation has also been used with SS-OCT. Wang et al. investigated 3D lamina cribrosa microarchitecture in 68 eyes (49 glaucomatous and 19 normals) using a SS-OCT device [67]. Larger beam thickness to pore diameter ratios and higher pore diameter standard deviations were observed in the glaucoma group, possibly reflecting beam remodelling in glaucomatous eyes, with axonal loss, reduction in pore size, and increased pore size variability [67]. Microarchitecture measurements of the lamina cribrosa using SS-OCT had good reproducibility with an imprecision of less than or equal to 4.2 % [68].

### Limitations of in vivo Evaluation of the Lamina Cribrosa

Despite the advances in lamina cribrosa imaging, current technology has several limitations. A major problem is the difficulty of visualizing the peripheral lamina due to blood vessels, scleral shadow, and broken images. Despite using algorithms to remove vascular shadows and enhance the contrast level of the images, most of the studies revealed significant rates of exclusion of lamina cribrosa images due to poor visualization, which may significantly limit the utility of in vivo lamina cribrosa imaging as a structural parameter to assess glaucomatous damage [33, 56]. Image quality will also decrease due to media opacities and small pupil size [69].

Current studies evaluating lamina cribrosa changes in glaucoma have primarily limited examined macro-architecture features using manual segmentation from OCT images, such as posterior displacement, lamina depth, and lamina thickness. However, manual delimitation of lamina cribrosa parameters may lead to subjective errors and imaging processing can be time consuming [33, 56]. Although automated segmentation methods have been



described, currently, there is no commercially available software for this purpose. Also, the lack of a normative database for lamina cribrosa parameters means one is unable to determine whether an individual exam is within normal limits or not. Variability in normal lamina cribrosa structure, for example, due to differences in axial length, may also limit the usefulness of lamina cribrosa as a diagnostic tool, unless it is used for longitudinal analysis. Moreover, to date, the evaluation of the lamina cribrosa in glaucoma has been limited to cross-sectional studies. Longitudinal studies are necessary to confirm the real usefulness of lamina cribrosa measurements in glaucoma management.

## Conclusion

Recent advances in imaging have significantly improved our ability to evaluate the lamina cribrosa in patients with glaucoma, providing a means to study the putative site of neural damage. There is growing evidence of association between lamina cribrosa structure and other structural and functional measures of glaucoma, which suggests that evaluation of the lamina cribrosa may prove a useful addition to clinical imaging options for detecting glaucoma and glaucoma progression. Lamina cribrosa imaging also has the potential to improve understanding of mechanisms of glaucomatous RGC injury, and although the temporal relationship between lamina cribrosa and neural changes remains uncertain, there is the possibility that lamina cribrosa changes may be a useful biomarker of increased risk of neural losses. Despite the promise of lamina cribrosa imaging in glaucoma management, further studies are needed. Particularly, there is a need for prospective studies evaluating lamina cribrosa changes over time and their relationship with glaucoma progression. The idea of expanding the algorithms to allow automated detection of lamina thickness and focal defects would also make testing more practical from a clinical standpoint. Despite these limitations, quantitative measurement of lamina cribrosa architecture is now possible, offering the potential to serve as a biomarker for glaucomatous damage and providing novel insights into this blinding disease.

**Acknowledgments** This article was supported in part by the National Institutes of Health/National Eye Institute grants EY021818 (F.A.M.), core grant P30EY022589; an unrestricted grant from Research to Prevent Blindness (New York, NY); fellowships from Brazilian National Research Council-CAPES 12309-13-3 (C.P.B.G.).

**Disclosure** Dr. Abe, Dr. Gracitelli, and Dr. Dimiz-Filho declare they have no conflicts of interest to declare. Dr. Tatham declares they received research support from Heidelberg Engineering. Dr. Medeiros declares they received research support from Alcon Laboratories, Bausch & Lomb, Carl Zeiss Meditec, Heidelberg Engineering, Merck,

Allergan, Sensimed, Topcon, Reichert, National Eye Institute; Consultant for Allergan, Carl Zeiss Meditec, Novartis.

**Human and Animal Rights and Informed Consent** This article contains no studies with human or animal subjects performed by the author.

## References

Papers of particular interest, published recently, have been highlighted as:

- Of importance
- Of major importance

1. Weinreb RN, Aung T, Medeiros FA. The pathophysiology and treatment of glaucoma: a review. *JAMA*. 2014;311:1901–11.
2. Minckler DS, Bunt AH, Johanson GW. Orthograde and retrograde axoplasmic transport during acute ocular hypertension in the monkey. *Invest Ophthalmol Vis Sci*. 1977;16:426–41.
3. Quigley HA, Addicks EM. Regional differences in the structure of the lamina cribrosa and their relation to glaucomatous optic nerve damage. *Arch Ophthalmol*. 1981;99:137–43.
4. Quigley HA, Addicks EM, Green WR, Maumenee AE. Optic nerve damage in human glaucoma. II. The site of injury and susceptibility to damage. *Arch Ophthalmol*. 1981;99:635–49.
5. Burgoyne CF, Downs JC, Bellezza AJ, Hart RT. Three-dimensional reconstruction of normal and early glaucoma monkey optic nerve head connective tissues. *Invest Ophthalmol Vis Sci*. 2004;45:4388–99.
6. Kass MA, Heuer DK, Higginbotham EJ, et al. The Ocular Hypertension Treatment Study: a randomized trial determines that topical ocular hypotensive medication delays or prevents the onset of primary open-angle glaucoma. *Arch Ophthalmol*. 2002;120:701–13 discussion 829–30.
7. Anderson DR, Drance SM, Schulzer M, Group CN-TGS. Factors that predict the benefit of lowering intraocular pressure in normal tension glaucoma. *Am J Ophthalmol*. 2003;136:820–9.
8. Anderson DR, Hendrickson A. Effect of intraocular pressure on rapid axoplasmic transport in monkey optic nerve. *Invest Ophthalmol*. 1974;13:771–83.
9. Gamero GE, Fechtner RD. The optic nerve in glaucoma. In: Choplin NT, Lundy DC, editors. *Atlas of Glaucoma*. London: Informa Healthcare; 2007. p. 59–74.
10. Burgoyne CF. A biomechanical paradigm for axonal insult within the optic nerve head in aging and glaucoma. *Exp Eye Res*. 2011;93:120–32.
11. Anderson DR. Ultrastructure of human and monkey lamina cribrosa and optic nerve head. *Arch Ophthalmol*. 1969;82:800–14.
12. Jonas JB, Mardin CY, Schlötzer-Schrehardt U, Naumann GO. Morphometry of the human lamina cribrosa surface. *Invest Ophthalmol Vis Sci*. 1991;32:401–5.
13. Strouthidis NG, Girard MJ. Altering the way the optic nerve head responds to intraocular pressure—a potential approach to glaucoma therapy. *Curr Opin Pharmacol*. 2013;13:83–9.
14. Crawford Downs J, Roberts MD, Sigal IA. Glaucomatous cupping of the lamina cribrosa: a review of the evidence for active progressive remodeling as a mechanism. *Exp Eye Res*. 2011;93:133–40.
15. Burgoyne CF, Downs JC, Bellezza AJ, Suh JK, Hart RT. The optic nerve head as a biomechanical structure: a new paradigm for understanding the role of IOP-related stress and strain in the

- pathophysiology of glaucomatous optic nerve head damage. *Prog Retin Eye Res.* 2005;24:39–73.
16. Burgoyne CF, Quigley HA, Thompson HW, Vitale S, Varma R. Early changes in optic disc compliance and surface position in experimental glaucoma. *Ophthalmology.* 1995;102:1800–9.
  17. Yan DB, Coloma FM, Metheetrairut A, et al. Deformation of the lamina cribrosa by elevated intraocular pressure. *Br J Ophthalmol.* 1994;78:643–8.
  18. Quigley HA, Hohman RM, Addicks EM, Massof RW, Green WR. Morphologic changes in the lamina cribrosa correlated with neural loss in open-angle glaucoma. *Am J Ophthalmol.* 1983;95:673–91.
  19. Jonas JB, Berenshtein E, Holbach L. Anatomic relationship between lamina cribrosa, intraocular space, and cerebrospinal fluid space. *Invest Ophthalmol Vis Sci.* 2003;44:5189–95.
  20. Morgan WH, Yu DY, Alder VA, et al. The correlation between cerebrospinal fluid pressure and retrolaminar tissue pressure. *Invest Ophthalmol Vis Sci.* 1998;39:1419–28.
  21. The Advanced Glaucoma Intervention Study (AGIS). 12. Baseline risk factors for sustained loss of visual field and visual acuity in patients with advanced glaucoma. *Am J Ophthalmol.* 2002;134:499–512.
  22. Ren R, Jonas JB, Tian G, et al. Cerebrospinal fluid pressure in glaucoma: a prospective study. *Ophthalmology.* 2010;117:259–66.
  23. Huang D, Swanson EA, Lin CP, et al. Optical coherence tomography. *Science.* 1991;254:1178–81.
  24. Wollstein G, Schuman JS, Price LL, et al. Optical coherence tomography longitudinal evaluation of retinal nerve fiber layer thickness in glaucoma. *Arch Ophthalmol.* 2005;123:464–70.
  25. Medeiros FA, Zangwill LM, Bowd C, et al. Evaluation of retinal nerve fiber layer, optic nerve head, and macular thickness measurements for glaucoma detection using optical coherence tomography. *Am J Ophthalmol.* 2005;139:44–55.
  26. Knight OJ, Chang RT, Feuer WJ, Budenz DL. Comparison of retinal nerve fiber layer measurements using time domain and spectral domain optical coherent tomography. *Ophthalmology.* 2009;116:1271–7.
  27. Kagemann L, Ishikawa H, Wollstein G, et al. Ultrahigh-resolution spectral domain optical coherence tomography imaging of the lamina cribrosa. *Ophthalmic Surg Lasers Imaging.* 2008;39:S126–31.
  28. Inoue R, Hangai M, Kotera Y, et al. Three-dimensional high-speed optical coherence tomography imaging of lamina cribrosa in glaucoma. *Ophthalmology.* 2009;116:214–22.
  29. Strouthidis NG, Grimm J, Williams GA, et al. A comparison of optic nerve head morphology viewed by spectral domain optical coherence tomography and by serial histology. *Invest Ophthalmol Vis Sci.* 2010;51:1464–74.
  30. Lin P, Mettu PS, Pomerleau DL, et al. Image inversion spectral-domain optical coherence tomography optimizes choroidal thickness and detail through improved contrast. *Invest Ophthalmol Vis Sci.* 2012;53:1874–82.
  31. Spaide RF, Koizumi H, Pozzoni MC, Pozzoni MC. Enhanced depth imaging spectral-domain optical coherence tomography. *Am J Ophthalmol.* 2008;146:496–500.
  32. Rebolleda G, Muñoz Negrete FJ. Enhanced depth imaging—optical coherence tomography technique and the lamina cribrosa in glaucoma. *Arch Soc Esp Oftalmol.* 2014;89:133–5.
  33. Park HY, Park CK. Diagnostic capability of lamina cribrosa thickness by enhanced depth imaging and factors affecting thickness in patients with glaucoma. *Ophthalmology.* 2013;120:745–52.
  34. Leung CK. Diagnosing glaucoma progression with optical coherence tomography. *Curr Opin Ophthalmol.* 2014;25:104–11.
  35. Yasuno Y, Hong Y, Makita S, et al. In vivo high-contrast imaging of deep posterior eye by 1-microm swept source optical coherence tomography and scattering optical coherence angiography. *Opt Express.* 2007;15:6121–39.
  36. Srinivasan VJ, Adler DC, Chen Y, et al. Ultrahigh-speed optical coherence tomography for three-dimensional and en face imaging of the retina and optic nerve head. *Invest Ophthalmol Vis Sci.* 2008;49:5103–10.
  37. Ivers KM, Li C, Patel N, et al. Reproducibility of measuring lamina cribrosa pore geometry in human and nonhuman primates with in vivo adaptive optics imaging. *Invest Ophthalmol Vis Sci.* 2011;52:5473–80.
  38. Akagi T, Hangai M, Takayama K, et al. In vivo imaging of lamina cribrosa pores by adaptive optics scanning laser ophthalmoscopy. *Invest Ophthalmol Vis Sci.* 2012;53:4111–9.
  39. Dreher AW, Bille JF, Weinreb RN. Active optical depth resolution improvement of the laser tomographic scanner. *Appl Opt.* 1989;28:804–8.
  40. Liang J, Williams DR, Miller DT. Supernormal vision and high-resolution retinal imaging through adaptive optics. *J Opt Soc Am A Opt Image Sci Vis.* 1997;14:2884–92.
  41. Miller DT, Kocaoglu OP, Wang Q, Lee S. Adaptive optics and the eye (super resolution OCT). *Eye (Lond).* 2011;25:321–30.
  42. Park SC, Kiumehr S, Dorairaj S, et al. In-vivo, 3-dimensional imaging of the lamina cribrosa horizontal central ridge in normals and lamina cribrosa deformation in glaucoma. *Invest Ophthalmol Vis Sci.* 2011;52:3063 E-Abstract.
  43. • Furlanetto RL, Park SC, Damle UJ, et al. Posterior displacement of the lamina cribrosa in glaucoma: in vivo interindividual and intereye comparisons. *Invest Ophthalmol Vis Sci.* 2013;54(7):4836–42. *In vivo human study, showing that lamina cribrosa was located more posteriorly in glaucoma patients comparing to normal subjects.*
  44. Ren R, Yang H, Gardiner SK, et al. Anterior lamina cribrosa surface depth, age, and visual field sensitivity in the Portland Progression Project. *Invest Ophthalmol Vis Sci.* 2014;55:1531–9.
  45. • Seo JH, Kim TW, Weinreb RN. Lamina cribrosa depth in healthy eyes. *Invest Ophthalmol Vis Sci.* 2014;55:1241–51. *Study in normal eyes using EDI-OCT showing a wide variation in normal lamina cribrosa depth. The study also found correlation between lamina depth with axial length and gender.*
  46. Cheung CY, Chen D, Wong TY, et al. Determinants of quantitative optic nerve measurements using spectral domain optical coherence tomography in a population-based sample of non-glaucomatous subjects. *Invest Ophthalmol Vis Sci.* 2011;52:9629–35.
  47. Kim TW, Kim M, Weinreb RN, et al. Optic disc change with incipient myopia of childhood. *Ophthalmology.* 2012;119:21–6 e1–3.
  48. Jonas JB, Berenshtein E, Holbach L. Lamina cribrosa thickness and spatial relationships between intraocular space and cerebrospinal fluid space in highly myopic eyes. *Invest Ophthalmol Vis Sci.* 2004;45:2660–5.
  49. Burgoyne CF, Morrison JC. The anatomy and pathophysiology of the optic nerve head in glaucoma. *J Glaucoma.* 2001;10:S16–8.
  50. Park HY, Jeon SH, Park CK. Enhanced depth imaging detects lamina cribrosa thickness differences in normal tension glaucoma and primary open-angle glaucoma. *Ophthalmology.* 2012;119:10–20.
  51. Park HY, Shin HY, Park CK. Imaging the posterior segment of the eye using swept-source optical coherence tomography in myopic glaucoma eyes: comparison with enhanced-depth imaging. *Am J Ophthalmol.* 2014;157:550–7.
  52. Kiumehr S, Park SC, Syril D, et al. In vivo evaluation of focal lamina cribrosa defects in glaucoma. *Arch Ophthalmol.* 2012;130:552–9.
  53. You JY, Park SC, Su D, et al. Focal lamina cribrosa defects associated with glaucomatous rim thinning and acquired pits. *JAMA Ophthalmol.* 2013;131:314–20.

54. Tatham AJ, Miki A, Weinreb RN, Zangwill LM, Medeiros FA. Defects of the lamina cribrosa in eyes with localized retinal nerve fiber layer loss. *Ophthalmology*. 2014;121:110–8.
55. Park SC, Hsu AT, Su D, et al. Factors associated with focal lamina cribrosa defects in glaucoma. *Invest Ophthalmol Vis Sci*. 2013;54:8401–7.
56. Lee EJ, Kim TW, Kim M, et al. Recent structural alteration of the peripheral lamina cribrosa near the location of disc hemorrhage in glaucoma. *Invest Ophthalmol Vis Sci*. 2014;55:2805–15.
57. Faridi OS, Park SC, Kabadi R, et al. Effect of focal lamina cribrosa defect on glaucomatous visual field progression. *Ophthalmology*. 2014;121:1524–30.
58. Wilkins MR, Fitzke FW, Khaw PT. Pointwise linear progression criteria and the detection of visual field change in a glaucoma trial. *Eye (Lond)*. 2006;20:98–106.
59. Maeda H, Nakamura M, Yamamoto M. Morphometric features of laminar pores in lamina cribrosa observed by scanning laser ophthalmoscopy. *Jpn J Ophthalmol*. 1999;43:415–21.
60. Miglior S, Rossetti L, Lonati C, Orzalesi N. Scanning laser ophthalmoscopy of the optic disc at the level of the lamina cribrosa. *Curr Eye Res*. 1998;17:453–61.
61. Miller KM, Quigley HA. The clinical appearance of the lamina cribrosa as a function of the extent of glaucomatous optic nerve damage. *Ophthalmology*. 1988;95:135–8.
62. Susanna R. The lamina cribrosa and visual field defects in open-angle glaucoma. *Can J Ophthalmol*. 1983;18:124–6.
63. Hermann B, Fernández EJ, Unterhuber A, et al. Adaptive-optics ultrahigh-resolution optical coherence tomography. *Opt Lett*. 2004;29:2142–4.
64. Zhang Y, Rha J, Jonnal R, Miller D. Adaptive optics parallel spectral domain optical coherence tomography for imaging the living retina. *Opt Express*. 2005;13:4792–811.
65. •• Nadler Z, Wang B, Wollstein G, et al. Automated lamina cribrosa microstructural segmentation in optical coherence tomography scans of healthy and glaucomatous eyes. *Biomed Opt Express*. 2013;4:2596–608. *Study showing that automated segmentation algorithm for in vivo imaging of the lamina cribrosa was similar to manual segmentation with the advantage of providing faster imaging analysis.*
66. Nadler Z, Wang B, Wollstein G, et al. Repeatability of in vivo 3D lamina cribrosa microarchitecture using adaptive optics spectral domain optical coherence tomography. *Biomed Opt Express*. 2014;5:1114–23.
67. Wang B, Nevins JE, Nadler Z, et al. In vivo lamina cribrosa micro-architecture in healthy and glaucomatous eyes as assessed by optical coherence tomography. *Invest Ophthalmol Vis Sci*. 2013;54:8270–4.
68. Wang B, Nevins JE, Nadler Z, et al. Reproducibility of in vivo OCT measured three-dimensional human lamina cribrosa microarchitecture. *PLoS ONE*. 2014;9:e95526.
69. Somfai GM, Salinas HM, Puliafito CA, Fernández DC. Evaluation of potential image acquisition pitfalls during optical coherence tomography and their influence on retinal image segmentation. *J Biomed Opt*. 2007;12:041209.